EM-Patroller: Entropy Maximized Multi-Robot Patrolling with Steady State Distribution Approximation

Hongliang Guo, Qi Kang, Wei-Yun Yau, Daniela Rus and Marcelo H. Ang Jr.

***Abstract*—This paper investigates the multi-robot patrolling (MuRP) problem in a discrete environment with the objective of approaching the uniform node coverage probability distribution by the robot team. Prevailing MuRP solutions for uniform node coverage either incur high (non-polynomial) computational complexity operations for the global optimal solution, or recourse to simple yet effective heuristics for approximate solutions without any performance guarantee. In this paper, we bridge the gap by proposing an efficient iterative algorithm, namely Entropy Maximized Patroller (EM-Patroller), with the per-iteration performance improvement guarantee and polynomial computational complexity. We reformulate the multi-robot patrolling problem in discrete environments as an 'unnormalized' joint steady state distribution entropy maximization problem, and employ multi-layer perceptron (MLP) to model the relationship between each robot's patrolling strategy and the individual steady state distribution. Then, we derive a multi-agent model-based policy gradient method to gradually update the robots' patrolling strategies towards the optimum. Complexity analysis indicates the polynomial computational complexity of EM-Patroller, and we also show that EM-Patroller has additional benefits of catering to miscellaneous user-defined joint steady state distributions and incorporating other objectives, *e.g.*, entropy maximization of individual steady state distribution, into the objective. We compare EM-Patroller with state-of-the-art MuRP algorithms in a range of canonical multi-robot patrolling environments, and also deploy it to a real multi-robot system for patrolling in a self-constructed indoor environment.**

***Index Terms*—un-normalized joint steady state distribution, multi-robot patrolling, multi-agent model-based policy gradient.**

I. Introduction

MULTI-ROBOT patrolling (MuRP) aims at protecting a physical environment by deploying multiple robots to persistently travel around it and perform local observations for security purposes [1]. MuRP has application potentials in various scenarios, such as surveillance and vigilance for regional security [2], [3], hazardous environment monitoring [4], [5], patrolling and disinfecting a COVID-19 infected area [6], [7]. Many of the aforementioned tasks are mundane, dangerous and/or costly for human beings, and thus they serve as well suited use cases for multi-robot systems (MRSs).

To date, researchers have developed various algorithms as MuRP solutions, and a brief literature review is provided in Section II. Here, we wish to articulate that prevailing MuRP methodologies for the uniform node coverage problem can be roughly categorized into two groups, namely (1) optimization methods, which formulate MuRP as a (multi-agent) travelling salesman problem (TSP), and incur non-polynomial computational complexity algorithms for the global optimal solution; and (2) heuristic algorithms, which design various local heuristics/rules to foster efficient multi-robot collaboration. Optimization methods are able to deliver the optimal solution at the cost of high computational complexity. On the other hand, heuristic algorithms yield simple yet effective patrolling strategies but cannot offer any global performance guarantee.

This paper aims at bridging the research gap by proposing an efficient optimization method, which guarantees the per-iteration performance improvement and meanwhile possesses polynomial computational complexity. Specifically, we propose an Entropy Maximized Patroller (EM-Patroller), which formulates MuRP for uniform node coverage as an *unnormalized* joint steady state distribution entropy maximization problem[1], and employs multi-layer perceptron (MLP) to model the relationship between each robot's patrolling strategy and the individual steady state distribution. We iteratively update the robot team's patrolling strategies through multi-agent model-based policy gradient and show that EM-Patroller has polynomial computational complexity and guarantees to improve the multi-robot patrolling performance iteration by iteration. Additionally, EM-Patroller has the flexibility of catering to miscellaneous user-defined target joint steady state distributions, *e.g.*, selectively put emphasis on a certain area's coverage probability, as well as incorporating other objectives, *e.g.*, the *individual* steady state distribution entropy maximization, into the objective. We will verify empirically that incorporating the individual steady state distribution entropy as an auxiliary optimization objective enhances EM-Patroller's robustness performance against individual failures. We evaluate and compare EM-Patroller's performance with state of the arts in a range of canonical MuRP environments, and also demonstrate the deployment process of EM-Patroller to a real multi-robot system in self-constructed indoor environments.

The contributions of this paper can be summarized as follows: (1) EM-Patroller serves as a polynomial computational complexity algorithm with the per-iteration performance improvement guarantee; (2) EM-Patroller has the flexibility of catering to miscellaneous user-defined joint steady state distribution instead of confining itself to unnormalized joint steady state entropy maximization; and (3) EM-Patroller exhibits great robustness performance against individual robot failures

[1]H. Guo, Q. Kang and WY. Yau are with Institute for Infocomm Research (I2R), Agency for Science, Technology and Research (A*STAR), 1 Fusionopolis Way, #21-01, Connexis South Tower, 138632, Republic of Singapore.

[3]D. Rus is with Computer Science and Artificial Intelligence Laboratory, Massachusetts Institute of Technology (MIT), Cambridge, MA 02139, USA.

[2]M. H. Ang is with National University of Singapore (NUS), Singapore.

[1]We will explain the rationale of selecting entropy maximization of the *unnormalized* joint steady state distribution as MuRP objective in Section III-B.

TABLE I
BIRD'S-EYE-VIEW OF THE MURP LITERATURE

Environments			Robot Models			Objectives				Methodologies		
Continuous	[8]–[12]	Comm. Models	robot-to-robot (R2R)	[8], [13]–[15]	Inherent	Minimize Idleness	Worst Idleness	[1], [8], [13], [14], [16]–[19]	Planning based	Offline	Global	[16], [20], [21]
Discrete	Grid World [15] [17]–[20] [22]–[25]		robot-to-environment (R2E)	[21]–[23] [26]–[30]			Mean Idleness	[15], [22], [26] [28], [31], [32]			Partitioned	[8]–[11] [13], [14] [18], [25], [31]
			robot-to-center (R2C)	[1], [20] [24], [33]			MFPT	[25], [34], [35]				
	Topology Graph [1], [13], [14] [16], [21] [26]–[33] [36], [37]		Decentralized (No Communication) [9]–[11], [16] [18], [25], [31], [36]			Approximate Frequency	Uniform Dist.	[15], [20], [27] [29], [32], [37]		Online	[17], [24]	
							Prioritized Dist.	[10], [11], [21]	Learning-based [22], [23], [26]–[28], [30]			
		Misc. Factors	Motion Constraint	[19]		Maximize Unpredictability	Entropy of Revisit	[38]				
			Motion Cost	[37]			Entropy Rate	[39]				
			Limited Visibility	[17], [25]	Intruder Oriented	Maximize Intruder Capture Probability		[40]–[42]	Heuristics [1], [15], [19], [29], [32], [36], [37]			
			Limited Endurance	[9], [10]		Maximize Intruder Detection Count		[36]				

when we incorporate the individual steady state distribution entropy maximization into the optimization objective.

II. LITERATURE REVIEW

This section presents a brief literature review of multi-robot patrolling along the taxonomies of (1) patrolling environments, (2) robot models, (3) objectives, and (4) mainstream methodologies. Table I displays a bird's-eye-view of MuRP literature and one is referred to [42], [43] for comprehensive reviews.

1) Patrolling Environments: In MuRP, the patrolling environments can be continuous [8]–[12], or discrete. For the discrete environment, it is either represented by a grid world [15], [17]–[20], [22]–[25], which functions as a straightforward way of transforming the continuous environments into discrete ones, or by a topological graph [1], [13], [14], [16], [21], [26]–[33], [36], [37], which merely describes the topological relationship between different areas of the environment.

2) Robot Models: First, the patrolling robots' communication models during online execution serve as one of the most crucial elements in fostering multi-robot collaboration for coordinated patrolling. We partition the robots' communication models into the following four categories, namely (1) robot-to-robot (R2R) communication [8], [13]–[15], [26]; (2) robot-to-environment (R2E) communication [21]–[23], [26]–[30]; (3) robot-to-center (R2C) communication [1], [20], [24], [33] and (4) purely decentralized (no communication) [9]–[11], [16], [18], [25], [31], [36]. In the meanwhile, researchers in the MuRP domain have also considered miscellaneous factors of the robots, *e.g.*, motion characteristics [19], motion cost [37], limited visibility [17], [25], fuel or battery life constraints [9], [10], into the MuRP-related algorithm design process.

3) Patrolling Objectives: Researchers have proposed various multi-robot patrolling objectives, and in this paper, we roughly categorize those objectives into two groups depending on whether the intruder's strategy influences the objective score or not, namely inherent MuRP objective, and intruder-oriented MuRP objective. The inherent MuRP objective does not depend on the intruder's characteristics, instead, it evaluates the MuRP system's performance based on internal characteristics, such as idleness, node visitation frequency, system's unpredictability. For example, idleness-related objectives include minimizing maximal/worst idleness [1], [8], [13], [14], [16]–[19], minimizing mean idleness [15], [22], [23], [26], [28], [31], [32], minimizing mean first-passage time (MFPT) [25], [34], [35]; node-visit frequency objectives include approaching uniform coverage frequency [15], [20], [27], [29], [32], [37], approximating the prioritized node-visit frequency [10], [11], [21]; and the unpredictability metric includes maximizing the entropy of return time (RT) [38], maximizing the average entropy rate [39]. On the other hand, intruder-oriented MuRP objectives evaluate the MuRP system's performance based on the statistics with respect to the intruder's behavior, *e.g.*, maximizing the intruder's capture probability within a given time budget [40]–[42], or maximizing the number of intruders being captured/detected within a given time horizon [36].

4) Mainstream Methodologies: This paper characterizes the mainstream methodologies for MuRP problem into three main categories, namely planning-based methods [18], [25], learning-based methods [22], [23] and heuristics [15], [32]. Planning-based methods typically formulate the MuRP problem into the mathematical optimization framework, and either incur off-the-shelf optimization solvers for offline planning solutions [8]–[11], [14], [16], [18], [20], [21], [25], [31] or receding horizon optimization tools [17], [24] for online replanning solutions. Depending on the nature of the formulated optimization problem, the robots' resulting patrolling strategies can be deterministic [8]–[11], [13], [14], [16]–[18], [20], [24], [31] or stochastic [21], [25], and the robots can be automatically allocated to separated regions within the environment [8]–[11], [13], [14], [18], [25], [31] or each robot is patrolling the whole environment with separated patrolling phases among team members [16], [17], [20], [21], [24].

Learning-based methods are deemed as recent emerging trends for MuRP solutions. They typically formulate the MuRP problem within the decentralized partial observable Markov decision process (Dec-POMDP) framework, and design the proper reward signal for each robot, so that the cumulative rewards represent (approximately) the MuRP system's overall objective. The majority of learning-based methods for MuRP target idleness-related objectives, and the reward signal is designed to reflect the instantaneous system-level idleness metric [23] or individual node-level idleness metric [22], [26]. For example, Jana *et al*. develop a deep Q-network (DQN)-based multi-robot patrolling algorithm, which is scalable to large-

scale graph environments, as the state-space encoding process is *independent* of the number of nodes in the graph [23]. The instantaneous reward signal for deep Q-network (DQN)-based multi-robot patrolling is defined as the ratio of instantiated local idleness to global idleness, and in this way, the robots are able to coordinate the minimize the system-level idleness so as to reach the maximal cumulative rewards.

The third category of methods designs various local heuristics/rules for effective and coordinated MuRP solutions. Each robot just follows the sometimes randomized decision-making policy based on certain pre-defined local rules for patrolling services, and the system will exhibit emerging collective performance. For example, Kappel *et al*. design and evaluate four local heuristic rules, namely watershed rule, time-based rule, evaporation heuristic, and communication-frequency strategy, to dispatch multiple UAVs for patrolling services, and demonstrate up-to-standard performance [15]. In general, designing heuristics for multi-robot patrolling is an effective and robust strategy, and is easy to implement. However, the algorithms in this category cannot establish a clear relationship between the local heuristics/rules and the system-level performance metric. Therefore, it is very difficult, if not impossible, to twist the heuristics for a fresh new MuRP objective metric.

This paper targets the MuRP problem of reaching a uniform node coverage probability. Planning methods for the uniform coverage objective usually incur non-polynomial computational complexity algorithms for the ultimate optimal solution, on the other hand, most learning-based methods struggle to design an appropriate local reward signal whose accumulation resembles the system-level uniform node coverage requirement. Lastly, for heuristics, the related algorithms are usually targeting the system-level *idleness-based* metric instead of uniform coverage, and it is impossible for the heuristic-based algorithms to yield iteration-by-iteration performance improvement guarantee, which is crucial in some critical MuRP application scenarios. Therefore, this paper aims at bridging the gap by proposing an efficient iterative optimization algorithm, which possesses both polynomial computational complexity and the per-iteration performance improvement guarantee.

III. Problem Formulation: multi-robot patrolling for Uniform Node Coverage

In this section, we present the mathematical problem formulation of multi-robot patrolling for uniform node coverage. We first introduce several new concepts in the MuRP problem, *i.e*., individual steady state distribution, node coverage probability, node coverage frequency, and joint steady state distribution, and then formulate the MuRP problem for uniform coverage as an unnormalized joint steady state distribution entropy maximization problem, followed by the specific objective selection rationale explanation.

A. MuRP Problem Setup

The multi-robot patrolling (MuRP) problem that we are considering in this paper is to coordinate a team of N mobile robots to persistently monitor a given discrete environment ($\mathcal{G}$) so that each node's *coverage probability* by the robot team is equal to each other, *i.e*., uniform coverage.

The patrolling environment is modeled as an undirected and connected unit-cost graph $\mathcal{G}(\mathcal{V}, \mathcal{E})$, where $\mathcal{V}$ ($|\mathcal{V}| = n$) refers to the set of nodes and $\mathcal{E}$ ($|\mathcal{E}| = m$) refers to the set of edges. The term 'unit-cost' means that $\forall(s, s') \in \mathcal{E}$, the transition time from node s to node s' is one unit time step for any robot in the multi-robot system. Note that the 'unit-cost' assumption of a graph $\mathcal{G}$ for the MuRP problem in discrete environments with the uniform coverage objective is a common scheme in the MuRP domain, see [15], [32] as examples. In practice, if we meet a 'long traversal' edge, one may simply divide it into several 'unit-cost' sub-edges and add the corresponding intermediate nodes into the node collection set ($\mathcal{V}$).

Definition 1 (Individual Steady State Distribution ($\boldsymbol{\mu}_i$))**.** The individual steady state distribution, denoted as $\boldsymbol{\mu}_i$ for robot i, is the stationary distribution of the Markov chain induced by π_i for Graph $\mathcal{G}$.

Note that, theoretically, the existence of stationary distribution of a Markov chain (MC), requires that the induced MC is *irreducible* and *aperiodic* [44]. However, in practice, we find that as long as the robot's starting policy induces an irreducible and aperiodic Markov chain, the following updated policies will satisfy the constraint automatically, with a small enough update step size. Therefore, we do not consider the existence of stationary distribution as an explicit constraint in the multi-agent model-based policy gradient's derivation process. With $\mu_i(s)$, we deliver the following two closely related but different concepts, namely the node coverage **probability** ($\mu(s)$) and the node coverage **frequency** ($\lambda(s)$).

Definition 2 (Node Coverage Probability (μ))**.** The coverage probability of a node s, *i.e*., $\mu(s)$, is defined as the probability that node s is visited by *any* robot per unit time step.

Definition 3 (Node Coverage Frequency (λ))**.** The coverage frequency of a node s, *i.e*., $\lambda(s)$, is defined as the average number of robots visiting node s per unit time step.

Note that $\mu(s)$ is, in most cases, not equal to $\lambda(s)$. With the individual steady state distribution $\boldsymbol{\mu}_i$, one may calculate the node coverage probability for node s as:

$$\mu(s) = 1 - \prod_{i=1}^{N}(1 - \mu_i(s)), \tag{1}$$

and the node coverage frequency for node s as:

$$\lambda(s) = \sum_{i=1}^{N} \mu_i(s), \tag{2}$$

where N is the total number of patrolling robots.

Definition 4 ((Unnormalized) Joint Steady State Distribution ($\boldsymbol{\mu}$))**.** The joint steady state distribution, denoted as $\boldsymbol{\mu}$ for the MRS, is the **unnormalized** node coverage probability vector, with each element referring to the node's coverage probability.

In Definition 4, the term 'unnormalized' means that in most cases $\sum_s \mu(s) \neq 1$.

B. MuRP Problem Formulation

The uniform node coverage MuRP problem is formulated as the following unnormalized entropy maximization problem:

$$\underset{\pi_1,\ldots,\pi_N}{\text{maximize}} \quad J = \sum_{s\in\mathcal{V}} -\mu(s)\log\big(\mu(s)\big). \tag{3}$$

Before proceeding to the multi-agent model-based policy gradient theorem in Section IV, we first lay down the rationale of selecting entropy maximization of the unnormalized joint steady state distribution as the objective function for MuRP.

Firstly, why do we choose the node coverage **probability** $\big(\mu(s)\big)$ over the node coverage **frequency** $\big(\lambda(s)\big)$ as the core evaluation ingredient in the objective function? In most of the multi-robot patrolling scenarios, the key criterion is whether a node has been visited or not $\big(\mu(s)\big)$ within a certain time period, instead of the average visit times $\big(\lambda(s)\big)$ within that time frame. Imagine a scenario, which is a ring of 6 nodes, and we are given 6 robots starting at the same node. If all the robots are circling the ring with the same pace, we have $\forall s \in \mathcal{V}$, $\mu(s) = 1/6$, in that the 6 robots 'conglomerate' together all the time, and the actual node coverage probability is $1/6$. However, $\lambda(s) = 1$, which means that *on average*, each node is visited 1.0 times during a unit time frame. Apparently, for this simple use case, letting each robot 'stay' on a distinct node is the optimal solution, which results in $\mu(s) = 1$. However, the solution still yields $\lambda(s) = 1$, which is the exactly the same as what we do to let the robots circle the ring with the same pace. Therefore, in the targeted MuRP problem, we use $\mu(s)$ instead of $\lambda(s)$ as the core evaluation ingredient.

Secondly, why do we use the rather complex (unnormalized) entropy of the joint steady state distribution to quantify the robot team's performance with the objective of uniform node coverage probability? A much more straightforward way of expressing the objective function is to minimize the variance of $\boldsymbol{\mu}$, *i.e.*, $\sum_s(\mu(s)-\bar{\mu}(s))^2$, where $\bar{\mu}(s) = \sum_s \mu(s)/n$, and n is the total number of nodes in $\mathcal{G}$. However, minimizing the variance of $\boldsymbol{\mu}$ will, sometimes, lead to a 'lazy' and meaningless solution. For example, we are given a discrete environment with n nodes, and N robots start at the robot depot, which does not count as a node. In this case, the robot team would select to stay at the depot, which results in $\mu(s) = 0$ for all the nodes. It is the optimal solution, as the variance of $\boldsymbol{\mu}$ is zero. However, the solution is meaningless, in that the robot team does not surveil the environment at all. On the other hand, when we express the objective as the entropy maximization of the joint steady state distribution, it automatically drives the robots' strategies towards a uniform distribution, in that the entropy is 'peaked' at the uniform distribution. In the meanwhile, we use the 'unnormalized' entropy expression, which tends to increase the the summation of $\mu(s)$ as well. In that the summation of $\mu(s)$ increases, the 'unnormalized' entropy value increases accordingly. Therefore, in this paper, we formulate the mathematical optimization objective as the 'unnormalized' entropy maximization of the joint steady state distribution, as stated in Eq. (3).

IV. Methodology

This section presents EM-Patroller as an efficient solution to MuRP for uniform node coverage. We first introduce the multi-agent model-based policy gradient theorem, which serves as the core of EM-Patroller to update each robot's policy parameters, and then present EM-Patroller's pseudo code and analyze its polynomial computational complexity with the big O notation. The section ends with displaying three main variants of the EM-Patroller, namely (1) robust EM-Patroller, (2) variational EM-Patroller, and (3) soft EM-Patroller.

A. Multi-Agent Model-based Policy Gradient

In this subsection, we derive the gradient of the objective function in Eq. (3), with respect to the parameterized individual policies. Before that, we first establish the relationship between $\boldsymbol{\mu}_i$ and $\pi_i(\boldsymbol{\theta}_i)$, where $\boldsymbol{\theta}_i \in \mathcal{R}^d$ refers to robot i's policy parameters.

Given a parameterized policy $\pi_i(\boldsymbol{\theta}_i)$, and the topological graph $\mathcal{G}$, one is able to calculate the state transition matrix of the policy-induced first-order Markov chain, and we represent the state transition matrix as $\boldsymbol{P}_{\boldsymbol{\theta}_i}$. In this case, the individual steady state distribution $\boldsymbol{\mu}_i$ satisfies that

$$\boldsymbol{P}_{\boldsymbol{\theta}_i}\boldsymbol{\mu}_i = \boldsymbol{\mu}_i. \tag{4}$$

Now, when given any $\boldsymbol{\theta}_i$, we are able to generate $\boldsymbol{P}_{\boldsymbol{\theta}_i}$, and then calculate $\boldsymbol{\mu}_i$ by solving Eq. (4) either analytically or iteratively. However, we need to calculate the gradient of $\boldsymbol{\mu}_i$ with respect to $\boldsymbol{\theta}_i$, *i.e.*, the Jacobian matrix $\partial\boldsymbol{\mu}_i/\partial\boldsymbol{\theta}_i$, which is one of the required inputs of the multi-agent model-based policy gradient.

In this paper, we treat the modeling process from $\boldsymbol{\theta}_i$ to $\boldsymbol{\mu}_i$ as a machine learning problem, and establish a multi-layer perceptron (MLP) which takes $\boldsymbol{\theta}_i$ as inputs and $\boldsymbol{\mu}_i$ as outputs, *i.e.*, $\boldsymbol{\mu}_i = \text{mlp}(\boldsymbol{\theta}_i)$. Since for any $\boldsymbol{\theta}_i$, we are able to calculate $\boldsymbol{\mu}_i$ with Eq. (4). It means that we can have as many training and testing samples as we need, and train the MLP to approximate the relationship between $\boldsymbol{\theta}_i$ and $\boldsymbol{\mu}_i$. With well-trained MLP, we can calculate the gradient of $\boldsymbol{\mu}_i$ with respect to $\boldsymbol{\theta}_i$, *i.e.*, $\partial\boldsymbol{\mu}_i/\partial\boldsymbol{\theta}_i$, with back-propagation.

With the available Jacobian matrix, *i.e.*, $\partial\boldsymbol{\mu}_i/\partial\boldsymbol{\theta}_i$, from the well-trained MLP, we present the multi-agent model-based policy gradient theorem as follows:

Theorem 1 (Multi-Agent Model-based Policy Gradient)**.** $\forall i \in \{1, 2, \ldots, N\}$, we have:

$$\boldsymbol{\nabla}_{\boldsymbol{\theta}_i} J = \sum_{s\in\mathcal{V}} (\log\mu(s) + 1)(1-\mu(s))\boldsymbol{\nabla}_{\boldsymbol{\theta}_i}\log(1-\mu_i(s)).$$

The proof process of Theorem 1 as depicted below is to make use of the chain rule of multi-variable calculus, and take advantage of the fact that $\forall j \neq i$, $\boldsymbol{\nabla}_{\boldsymbol{\theta}_i}\mu_j(s) = \mathbf{0}$.

Proof.

$$
\begin{aligned}
&\nabla_{\boldsymbol{\theta}_i} J \\
=&\sum_{s\in\mathcal{V}} \Big(\frac{\partial J}{\partial \mu(s)} \times \sum_{j=1}^{N} \big(\frac{\partial \mu(s)}{\partial \mu_j(s)} \times \frac{\partial \mu_j(s)}{\partial \boldsymbol{\theta}_i} \big) \Big) \\
=&\sum_{s\in\mathcal{V}} \sum_{j=1}^{N} \frac{\partial J}{\partial \mu(s)} \times \frac{\partial \mu(s)}{\partial \mu_j(s)} \times \frac{\partial \mu_j(s)}{\partial \boldsymbol{\theta}_i} \\
=&\sum_{s\in\mathcal{V}} \sum_{j\neq i} \frac{\partial J}{\partial \mu(s)} \frac{\partial \mu(s)}{\partial \mu_j(s)} \frac{\partial \mu_j(s)}{\partial \boldsymbol{\theta}_i} + \sum_{s\in\mathcal{V}} \frac{\partial J}{\partial \mu(s)} \frac{\partial \mu(s)}{\partial \mu_i(s)} \frac{\partial \mu_i(s)}{\partial \boldsymbol{\theta}_i} \\
=&\sum_{s\in\mathcal{V}} \frac{\partial J}{\partial \mu(s)} \frac{\partial \mu(s)}{\partial \mu_i(s)} \frac{\partial \mu_i(s)}{\partial \boldsymbol{\theta}_i} \\
=&\sum_{s\in\mathcal{V}} -(\log \mu(s) + 1) \times \prod_{j=1, j\neq i}^{N} (1 - \mu_j(s)) \times \frac{\partial \mu_i(s)}{\partial \boldsymbol{\theta}_i} \\
=&\sum_{s\in\mathcal{V}} -(\log \mu(s) + 1) \times \frac{\prod_{j=1}^{N} (1 - \mu_j(s))}{1 - \mu_i(s)} \times \frac{\partial \mu_i(s)}{\partial \boldsymbol{\theta}_i} \\
=&\sum_{s\in\mathcal{V}} -(\log \mu(s) + 1) \times \frac{1 - \mu(s)}{1 - \mu_i(s)} \times \frac{\partial \mu_i(s)}{\partial \boldsymbol{\theta}_i} \\
=&\sum_{s\in\mathcal{V}} (\log \mu(s) + 1)(1 - \mu(s)) \nabla_{\boldsymbol{\theta}_i} \log(1 - \mu_i(s)) \qquad (5)
\end{aligned}
$$

□

B. Pseudo Code and Computational Complexity Analysis

With the multi-agent model-based policy gradient theorem, we deliver the training process of EM-Patroller in Algorithm 1. Next, we use the big O notation [45] to analyze the computational complexity of EM-Patroller's training process. Examining Algorithm 1, we find that the core computation happens between Line 2 and Line 12, which consists of three loops. For the first loop, both Line 3 and Line 4 have the $\mathcal{O}(1)$ complexity. Line 5 involves solving Eq. (4), and has $\mathcal{O}(n^3)$ complexity regardless of an analytic or iterative solution strategy. In summary, the first loop has $\mathcal{O}(n^3 N)$ complexity. Similar analysis can be applied to evaluate the computational complexity of the second and third loop, and we get $\mathcal{O}(n(N + Ndh))$, where h is the number of hidden nodes in MLP and $\mathcal{O}(N)$, respectively. Summing up the complexity for the three loops and ignoring all terms except for the leading ones, we get EM-Patroller's computational complexity at $\mathcal{O}\big((n^3 + n \times d \times h) \times N \times T_{\max}\big)$, which is polynomial with respect to number of robots (N) and scale of the graph (n).

Besides the polynomial computational complexity, EM-Patroller also possesses the characteristic of per-iteration performance improvement guarantee. The underlying rationale is that since the objective function (J)'s gradient has been derived with Theorem 1, when we set the learning rate α to be sufficiently small, the per-iteration update of individual policy parameters ($\boldsymbol{\theta}_i$) along J's gradient direction will increase the objective value. Furthermore, from Algorithm 1, we can see that there is no sampling process during the gradient calculation process, which means that the individual policy's parameter update is truly gradient ascent rather than *stochastic* gradient ascent. Due to the universal approximation ability of MLP, it is able to approximate the true relationship between $\boldsymbol{\mu}_i$ and $\boldsymbol{\theta}_i$ with arbitrary accuracy. Therefore, EM-Patroller possesses the per-iteration performance improvement guarantee.

Algorithm 1: Training Process of EM-Patroller

Input: Graph $\mathcal{G}$; number of robots N; pre-trained MLP for $\mathcal{G}$, *i.e.*, $\forall i \in \{1, 2, \ldots, N\}$, $\boldsymbol{\mu}_i = \text{mlp}(\boldsymbol{\theta}_i)$; max. training epoch: $T_{\max}$; learning rate α;
Output: Parameterized individual policy for each robot, *i.e.*, $\forall i \in \{1, 2, \ldots, N\}$, $\pi_i(\boldsymbol{\theta}_i)$;
Init: Randomly initialized policy parameters: $\forall i \in \{1, 2, \ldots, N\}$, $\boldsymbol{\theta}_i \in \mathcal{R}^d$; $t \leftarrow 0$;

1 **while** $t \leq T_{\max} - 1$ **do**
2 **foreach** $i \in \{1, 2, \ldots, N\}$ **do**
3 $\nabla_{\boldsymbol{\theta}_i} J \leftarrow \mathbf{0}$;
4 Calculate $\boldsymbol{P}_{\boldsymbol{\theta}_i}$ based on $\mathcal{G}$;
5 Calculate and store the individual steady state distribution $\boldsymbol{\mu}_i$ by solving Eq. (4) either analytically or iteratively;
6 **foreach** $s \in \mathcal{V}$ **do**
7 Calculate $\mu(s)$ based on $\mu_i(s)$ through Eq. (1);
8 **foreach** $i \in \{1, 2, \ldots, N\}$ **do**
9 Calculate $\nabla_{\boldsymbol{\theta}_i} \log(1 - \mu_i(s))$;
10 $\nabla_{\boldsymbol{\theta}_i} J \leftarrow \nabla_{\boldsymbol{\theta}_i} J + (\log \mu(s) + 1)(1 - \mu(s)) \nabla_{\boldsymbol{\theta}_i} \log(1 - \mu_i(s))$;
11 **foreach** $i \in \{1, 2, \ldots, N\}$ **do**
12 $\boldsymbol{\theta}_i \leftarrow \boldsymbol{\theta}_i + \alpha \cdot \nabla_{\boldsymbol{\theta}_i} J$;
13 $t \leftarrow t + 1$;
14 Final.

C. Variations of EM-Patroller

In this subsection, we briefly discuss three main variants of EM-Patroller, namely robust EM-Patroller, variational EM-Patroller and soft EM-Patroller.

1) Robust EM-Patroller: To increase the EM-Patroller's robustness against individual failures, *i.e.*, the individual robot malfunctions and completely quits the MuRP task, we augment EM-Patroller with an auxiliary objective, which targets maximizing the *individual* uniform coverage property. Specifically, we design $J_r = -\frac{1}{N} \sum_{i=1}^{N} \sum_{s\in\mathcal{V}} \mu_i(s) \log \mu_i(s)$ as the auxiliary objective, and define $J + \alpha_r J_r$, where $\alpha_r \geq 0$, as the augmented objective function, then we get the robust EM-Patroller. The rationale behind a robust EM-Patroller is that although some robots in the MRS malfunction and quit the team during execution, since each of the remaining robots is having an auxiliary uniform coverage objective, the remaining MRS will still exhibit the uniform node coverage property.

2) Variational EM-Patroller: Suppose that we have a specific multi-robot patrolling task, which has *prioritized* regions

(nodes) to be covered higher probabilities instead of the uniform node coverage. Defining the target joint steady state distribution as $\boldsymbol{\mu}'$, which is not necessarily a uniform distribution, we can formulate the new objective as minimizing the unnormalized Kullback–Leibler divergence (KL divergence) [46] from $\boldsymbol{\mu}$ to $\boldsymbol{\mu}'$, *i.e.*, $D_{\mathrm{KL}}(\boldsymbol{\mu} \parallel \boldsymbol{\mu}')$. After derivation, we can define $\tilde{J} = -D_{\mathrm{KL}}(\boldsymbol{\mu} \parallel \boldsymbol{\mu}') = -\sum_{s\in\mathcal{V}} \mu(s)\log(\mu(s)/\mu'(s))$ as the new objective function. Note that when we designate $\boldsymbol{\mu}'$ as the uniform distribution, variational EM-Patroller recovers to the canonical EM-Patroller.

3) Soft EM-Patroller: Another desired property for a MuRP algorithm is that it is 'unpredictable' from the observers'/intruders' perspective. We do not want to robots to regularly surveil the environment with a certain predictable pattern, in which case, the adversarial intruder will take advantage of the surveillance pattern, and attack the environment. In this paper, we gauge the unpredictability metric with the averaged expected entropy rate. Here, the entropy rate at node s for robot i refers to the entropy of robot i's policy at s. In this case, the auxiliary objective is defined as $J_s = -\frac{1}{N}\sum_{i=1}^{N}\sum_{s\in\mathcal{V}}\left(\mu_i(s)\sum_a \pi_i(a|s)\log\pi_i(a|s)\right)$. We define $J + \alpha_s J_s$, where $\alpha_s \geq 0$, as the augmented objective function, and the resulting solution is a soft EM-Patroller. Note that the term 'soft' comes from soft actor critic [47], whose auxiliary objective is to maximize the expected entropy of the agent's policy.

V. Simulation Results and Analysis

In this section, we benchmark EM-Patroller's performance with state of the arts in a range of canonical MuRP environments. For state of the arts, we select (1) multiple travelling salesman problem with spectral clustering (mTSP-SC) [18]; (2) DQN-Patroller [23]; (3) weighted node counting (w-NC) [32]; (4) PatrolGRAPH* [21] and (5) PatrolGRAPH^A [29]. Note that mTSP-SC, DQN-Patroller and w-NC serve as the most recent MuRP solutions along the categories of planning, learning and heuristics, respectively. We twist DQN-Patroller fit to topological environments by enlarging the action space to contain all valid edges in Graph $\mathcal{G}$, instead of confining it to four actions in the original paper.

The hyperparameters for EM-Patroller and state of the arts are configured as follows: (1) EM-Patroller[2]: $\alpha = 1\times10^{-4}$, $\alpha_r = 1.0$, $\alpha_s = 2.0$; (2) DQN-Patroller: $\alpha = 7.5\times10^{-4}$, $\gamma = 0.95$, $\epsilon = 0.93\times0.992^K$, where K is the number of episodes; (3) PatrolGRAPH*: $\sigma = 0.01$; (4) PatrolGRAPH^A: $K_1 = 1.0$, $K_2 = 10.0$, $\epsilon = 1\times10^{-8}$. Note that mTSP-SC and w-NC are free of hyperparameters. All algorithms are implemented in Python3.8 with publicly available source code[3], and all tests are executed on an 8 core CPU, 32GB RAM cloud computer with the NVIDIA Tesla V100 and 64-bit Ubuntu system.

In the following three subsections, we first showcase the per-iteration improvement process of EM-Patroller in a simple yet illustrative environment, namely HOUSE, and then compare the performance of EM-Patroller with state of the arts in two canonical MuRP environments, namely MUSEUM and OFFICE. Finally, we evaluate the performance of robust EM-Patroller, variational EM-Patroller and soft EM-Patroller, with regard to their respective characteristics.

A. Performance Illustration in a Simple Environment

This subsection illustrates the per-iteration performance improvement characteristic of EM-Patroller in a simple environment, namely HOUSE, whose topology is shown in Fig. 1(a).

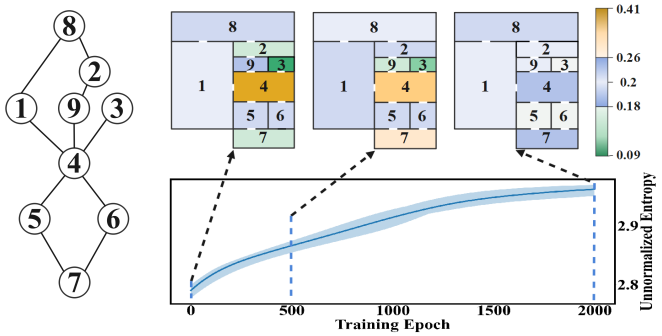

(a) House Topo. (b) Entropy Evolution Process and Heat Maps

Fig. 1. Training process of EM-Patroller in 'HOUSE' Environment, with $N = 2$ robots. The shaded area in bottom half of Fig. 1(b) indicates the standard deviation for differently initialized policy parameters. **All figures are best viewed in color**.

We configure two robots (both starts at node 4) with randomly initialized policy parameters, $\boldsymbol{\theta}_i$, and train EM-Patroller for 2000 epochs/iterations. The bottom half of Fig. 1(b) shows the evolution process of the joint steady state distribution's (unnormalized) entropy, which reflects its uniformity, and the top half of Fig. 1(b) visualizes the representative heat maps at Epoch 1, Epoch 500 and Epoch 2000, respectively. We can see that as the training process continues, the joint steady state distribution gradually approaches the uniform distribution.

B. Performance Comparison with State of the Arts

This subsection compares EM-Patroller with state of the arts in terms of the unnormalized entropy of the joint steady state distribution, *i.e.*, the value of J in Eq. (3), in two canonical MuRP environments, namely MUSEUM and OFFICE, as visualized in Fig. 2. Note that MUSEUM and OFFICE are two canonical MuRP problem testing environments, and they are abstractly represented by 'unit-cost' topological graphs.

We let the robots start at node 1 in MUSEUM and node 43 in OFFICE, and patrol the respective environment for uniform coverage. Fig. 3 shows the comparison results, where we can see that EM-Patroller achieves the best performance (gauged by the un-normalized entropy: J) in both environments for a variety of team sizes. Here, we wish to note that mTSP-SC calculates the optimal *deterministic* policies, which performs consistently better than DQN-Patroller, in that DQN-Patroller also outputs deterministic policies. However, EM-Patroller and other state of the arts yield *stochastic* patrolling policies, which

[2]Due to space limitations, we skip the ablation study results of EM-Patroller's hyper-parameters, *i.e.*, α, α_r, α_s, and directly display the final settings. Interested audiences are referred to the code repository for details.

[3]Code repository: https://github.com/kevinkang1125/EM-Patroller

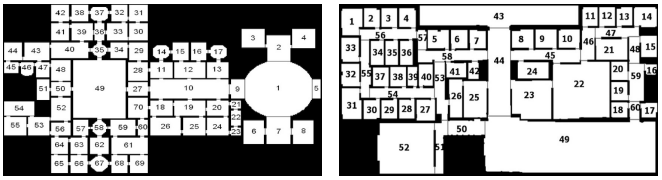

(a) MUSEUM (b) OFFICE

Fig. 2. Canonical MuRP test environments from [48], each room is associated with the corresponding node number. Left: MUSEUM; Right: OFFICE

have the potential to outperform mTSP-SC. We construct a simple yet illustrative one-robot patrolling task, which favors the stochastic patrolling policy over deterministic ones, and audiences are referred to the code repository for details.

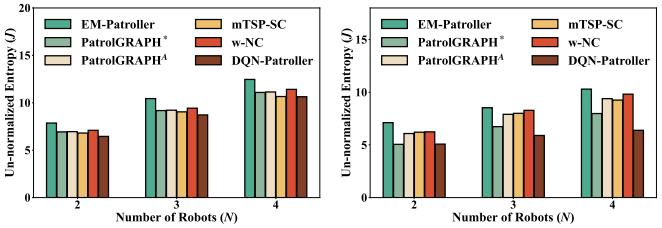

(a) MUSEUM Environment (b) OFFICE Environment

Fig. 3. Performance comparison with state of the arts in MUSEUM and OFFICE. Y-axis corresponds to the unnormalized entropy defined in Eq. (3)

C. Evaluation of EM-Patroller's Variations

This subsection evaluates the performance of robust EM-Patroller, variational EM-Patroller and soft EM-Patroller in MUSEUM and OFFICE. We gauge robustness as the percentage of the system's performance when one robot quits the team to the normal system's performance. Fig. 4(a) shows robustness comparisons between the canonical EM-Patroller and robust EM-Patroller. Fig. 4(b) visualizes the convergence processes of KL divergence for variational EM-Patroller in both environments, when we pick 4 prioritized nodes and double the corresponding importance weights. Fig. 4(c) shows the evolution process of the unpredictability (gauged by the averaged entropy rate) for soft EM-Patroller with respect to different number of robots in both MuRP environments.

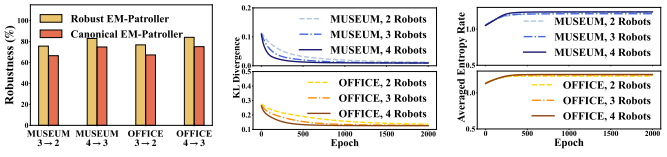

(a) Robust (b) Variational (c) Soft

Fig. 4. Performance evaluation of EM-Patroller's variations in terms of (1) robustness; (2) KL divergence; (3) un-predictability (averaged entropy rate).

VI. System Integration and Experimental Results

This section deploys EM-Patroller to a real multi-robot system and demonstrates its functionality in a self-constructed indoor environment. The patrolling robots are DM3008 robots[4] as shown in Fig. 5(a). DM3008 is a differential drive robot, with an embedded single beam LiDAR (LDS-50C-2) for map construction and obstacle detection. The product offers the simultaneous localization and mapping (SLAM) functionality, as well as an autonomous navigation module, which navigates the robot within a pre-constructed map while avoiding obstacles.

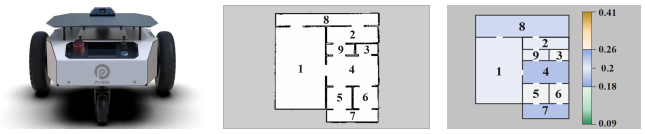

(a) DM3008 Robot (b) Constructed Map (c) Final Heat Map

Fig. 5. The patrolling robot testbed, constructed map and the final heat map.

We integrate EM-Patroller, which functions as an intermediate sub-goal generator, to DM3008, and evaluate EM-Patroller's performance through visualizing the joint steady state distribution. The indoor environment mimics the 'HOUSE' environment, whose constructed map is shown in Fig. 5(b). We deploy two DM3008 robots for patrolling, and execute 2000 consecutive time steps. The heat map of the environment's unnormalized coverage probability are shown in Fig. 5(c). From Fig. 5(c), we can see that EM-Patroller approaches, more or less, the uniform coverage of the environment. A demonstration video is uploaded with the main manuscript, and more videos are available in the previously referred code repository.

VII. Conclusion and Future Work

This paper proposes EM-Patroller for the uniform node coverage MuRP problem. EM-Patroller enjoys both the polynomial computational complexity and the per-iteration performance improvement guarantee. We compare EM-Patroller with state of the arts in two canonical MuRP environments, and also deploy it to real autonomous robot testbeds for demonstration in a self-constructed indoor environment. In the future, we would like to design the model-free version of EM-Patroller, which does not need the explicit modeling process between parameterized policies and the individual steady state distribution. In the meanwhile, we are also keen on incorporating intruder-based objectives into EM-Patroller.

References

[1] A. Machado, A. Almeida, G. Ramalho, J.-D. Zucker, and A. Drogoul, "Multi-agent movement coordination in patrolling," in *International Conference on Computer and Game*, 2002, pp. 155–170.

[2] J. Yang, Z. Ding, and L. Wang, "The programming model of air-ground cooperative patrol between multi-UAV and police car," *IEEE Access*, vol. 9, pp. 134 503–134 517, 2021.

[3] F. Dong, S. Fang, and Y. Xu, "Design and implementation of security robot for public safety," in *International Conference on Virtual Reality and Intelligent Systems (ICVRIS)*. IEEE, 2018, pp. 446–449.

[4] Q. An, X. Chen, and F. Liu, "Research and application of hazardous chemicals monitoring technology based on big data and patrol robot," in *Asia Conference on Information Engineering (ACIE)*. IEEE, 2022, pp. 5–9.

[4]More details about DM3008 are available from www.puweii.com.

[5] W. Rahmaniar and A. Wicaksono, "Design and implementation of a mobile robot for carbon monoxide monitoring," *Journal of Robotics and Control (JRC)*, vol. 2, no. 1, pp. 1–6, 2021.

[6] A. Khamis, J. Meng, J. Wang, A. T. Azar, E. Prestes, Á. Takács, I. J. Rudas, and T. Haidegger, "Robotics and intelligent systems against a pandemic," *Acta Polytechnica Hungarica*, vol. 18, no. 5, pp. 13–35, 2021.

[7] Z. Zhao, Y. Ma, A. Mushtaq, A. M. A. Rajper, M. Shehab, A. Heybourne, W. Song, H. Ren, and Z. T. H. Tse, "Applications of robotics, artificial intelligence, and digital technologies during COVID-19: a review," *Disaster Medicine and Public Health Preparedness*, pp. 1–11, 2021.

[8] J. J. Acevedo, B. Arrue, J. M. Diaz-Banez, I. Ventura, I. Maza, and A. Ollero, "Decentralized strategy to ensure information propagation in area monitoring missions with a team of UAVs under limited communications," in *IEEE International Conference on Unmanned Aircraft Systems (ICUAS)*. IEEE, 2013, pp. 565–574.

[9] D. Mitchell, M. Corah, N. Chakraborty, K. Sycara, and N. Michael, "Multi-robot long-term persistent coverage with fuel constrained robots," in *IEEE International Conference on Robotics and Automation (ICRA)*. IEEE, 2015, pp. 1093–1099.

[10] V. Mersheeva and G. Friedrich, "Multi-UAV monitoring with priorities and limited energy resources," in *International Conference on Automated Planning and Scheduling (ICAPS)*, vol. 25, 2015, pp. 347–355.

[11] V. Sea, A. Sugiyama, and T. Sugawara, "Frequency-based multi-agent patrolling model and its area partitioning solution method for balanced workload," in *International Conference on the Integration of Constraint Programming, Artificial Intelligence, and Operations Research (CPAIOR)*. Springer, 2018, pp. 530–545.

[12] C. Banerjee, D. Datta, and A. Agarwal, "Chaotic patrol robot with frequency constraints," in *IEEE International Conference on Research in Computational Intelligence and Communication Networks (ICRCICN)*. IEEE, 2015, pp. 340–344.

[13] F. Pasqualetti, A. Franchi, and F. Bullo, "On cooperative patrolling: Optimal trajectories, complexity analysis, and approximation algorithms," *IEEE Transactions on Robotics (T-RO)*, vol. 28, no. 3, pp. 592–606, 2012.

[14] F. Pasqualetti, J. W. Durham, and F. Bullo, "Cooperative patrolling via weighted tours: Performance analysis and distributed algorithms," *IEEE Transactions on Robotics (T-RO)*, vol. 28, no. 5, pp. 1181–1188, 2012.

[15] K. S. Kappel, T. M. Cabreira, J. L. Marins, L. B. de Brisolara, and P. R. Ferreira, "Strategies for patrolling missions with multiple UAVs," *Journal of Intelligent & Robotic Systems (JINT)*, vol. 99, no. 3, pp. 499–515, 2020.

[16] Y. Chevaleyre, "Theoretical analysis of the multi-agent patrolling problem," in *IEEE International Conference on Intelligent Agent Technology (IAT)*. IEEE, 2004, pp. 302–308.

[17] J. Scherer and B. Rinner, "Multi-robot persistent surveillance with connectivity constraints," *IEEE Access*, vol. 8, pp. 15 093–15 109, 2020.

[18] L. Collins, P. Ghassemi, E. T. Esfahani, D. Doermann, K. Dantu, and S. Chowdhury, "Scalable coverage path planning of multi-robot teams for monitoring non-convex areas," in *IEEE International Conference on Robotics and Automation (ICRA)*. IEEE, 2021, pp. 7393–7399.

[19] N. Nigam, S. Bieniawski, I. Kroo, and J. Vian, "Control of multiple UAVs for persistent surveillance: Algorithm and flight test results," *IEEE Transactions on Control Systems Technology (TCST)*, vol. 20, no. 5, pp. 1236–1251, 2011.

[20] Y. Elmaliach, N. Agmon, and G. A. Kaminka, "Multi-robot area patrol under frequency constraints," *Annals of Mathematics and Artificial Intelligence*, vol. 57, no. 3, pp. 293–320, 2009.

[21] G. Cannata and A. Sgorbissa, "A minimalist algorithm for multirobot continuous coverage," *IEEE Transactions on Robotics (T-RO)*, vol. 27, no. 2, pp. 297–312, 2011.

[22] S. Y. Luis, D. G. Reina, and S. L. T. Marín, "A multiagent deep reinforcement learning approach for path planning in autonomous surface vehicles: The Ypacaraí lake patrolling case," *IEEE Access*, vol. 9, pp. 17 084–17 099, 2021.

[23] M. Jana, L. Vachhani, and A. Sinha, "A deep reinforcement learning approach for multi-agent mobile robot patrolling," *International Journal of Intelligent Robotics and Applications (IJIRA)*, pp. 1–22, 2022.

[24] N. Rezazadeh and S. S. Kia, "A sub-modular receding horizon approach to persistent monitoring for a group of mobile agents over an urban area," in *IFAC Workshop on Distributed Estimation and Control in Networked Systems NECSYS*, vol. 52, no. 20. Elsevier, 2019, pp. 217–222.

[25] T. Alam, M. M. Rahman, P. Carrillo, L. Bobadilla, and B. Rapp, "Stochastic multi-robot patrolling with limited visibility," *Journal of Intelligent & Robotic Systems (JINT)*, vol. 97, no. 2, pp. 411–429, 2020.

[26] H. Santana, G. Ramalho, V. Corruble, and B. Ratitch, "Multi-agent patrolling with reinforcement learning," in *International Joint Conference on Autonomous Agents and Multiagent Systems (AAMAS)*, vol. 4. IEEE Computer Society, 2004, pp. 1122–1129.

[27] T. Mao and L. Ray, "Frequency-based patrolling with heterogeneous agents and limited communication," *arXiv preprint arXiv:1402.1757*, 2014.

[28] D. Portugal and R. P. Rocha, "Cooperative multi-robot patrol with Bayesian learning," *Autonomous Robots (AR)*, vol. 40, no. 5, pp. 929–953, 2016.

[29] G. Cannata and A. Sgorbissa, "A distributed, real-time approach to multi robot uniform frequency coverage," in *International Symposium on Distributed Autonomous Robotic Systems (DARS)*. Springer, 2013, pp. 19–32.

[30] X. Zhou, W. Wang, T. Wang, Y. Lei, and F. Zhong, "Bayesian reinforcement learning for multi-robot decentralized patrolling in uncertain environments," *IEEE Transactions on Vehicular Technology (T-VT)*, vol. 68, no. 12, pp. 11 691–11 703, 2019.

[31] Y. Hong, Y. Kyung, and S.-L. Kim, "A multi-robot cooperative patrolling algorithm with sharing multiple cycles," in *European Conference on Networks and Communications (EuCNC)*. IEEE, 2019, pp. 300–304.

[32] P. A. Sampaio and K. F. d. S. da Silva, "Decentralized strategies based on node marks for multi-robot patrolling on weighted graphs," in *Latin American Robotics Symposium (LARS)*. IEEE, 2019, pp. 317–322.

[33] S. Hoshino and K. Takahashi, "Dynamic partitioning strategies for multi-robot patrolling systems," *Journal of Robotics and Mechatronics (JRM)*, vol. 31, no. 4, pp. 535–545, 2019.

[34] P. Agharkar, R. Patel, and F. Bullo, "Robotic surveillance and Markov chains with minimal first passage time," in *IEEE Conference on Decision and Control (CDC)*. IEEE, 2014, pp. 6603–6608.

[35] R. Patel, P. Agharkar, and F. Bullo, "Robotic surveillance and Markov chains with minimal weighted Kemeny constant," *IEEE Transactions on Automatic Control (TAC)*, vol. 60, no. 12, pp. 3156–3167, 2015.

[36] T. Sak, J. Wainer, and S. K. Goldenstein, "Probabilistic multiagent patrolling," in *Brazilian Symposium on Artificial Intelligence*. Springer, 2008, pp. 124–133.

[37] M. Baglietto, G. Cannata, F. Capezio, and A. Sgorbissa, "Multi-robot uniform frequency coverage of significant locations in the environment," in *International Symposium on Distributed Autonomous Robotic Systems (DARS)*. Springer, 2009, pp. 3–14.

[38] X. Duan, M. George, and F. Bullo, "Markov chains with maximum return time entropy for robotic surveillance," *IEEE Transactions on Automatic Control (TAC)*, vol. 65, no. 1, pp. 72–86, 2019.

[39] M. George, S. Jafarpour, and F. Bullo, "Markov chains with maximum entropy for robotic surveillance," *IEEE Transactions on Automatic Control (TAC)*, vol. 64, no. 4, pp. 1566–1580, 2018.

[40] A. B. Asghar and S. L. Smith, "Stochastic patrolling in adversarial settings," in *2016 American Control Conference (ACC)*. IEEE, 2016, pp. 6435–6440.

[41] N. Basilico and S. Carpin, "Balancing unpredictability and coverage in adversarial patrolling settings," in *International Workshop on the Algorithmic Foundations of Robotics*. Springer, 2018, pp. 762–777.

[42] X. Duan, D. Paccagnan, and F. Bullo, "Stochastic strategies for robotic surveillance as stackelberg games," *IEEE Transactions on Control of Network Systems (TCNS)*, vol. 8, no. 2, pp. 769–780, 2021.

[43] N. Basilico, "Recent trends in robotic patrolling," *Current Robotics Reports*, pp. 1–12, 2022.

[44] P. Gagniuc, *Markov Chains: From Theory to Implementation and Experimentation*. John Wiley & Sons, 2017.

[45] D. E. Knuth, "Big omicron and big omega and big theta," *ACM Sigact News*, vol. 8, no. 2, pp. 18–24, 1976.

[46] S. Kullback and R. A. Leibler, "On Information and Sufficiency," *The Annals of Mathematical Statistics*, vol. 22, no. 1, pp. 79 – 86, 1951.

[47] T. Haarnoja, A. Zhou, P. Abbeel, and S. Levine, "Soft actor-critic: Off-policy maximum entropy deep reinforcement learning with a stochastic actor," in *International Conference on Machine Learning (ICML)*, J. Dy and A. Krause, Eds., vol. 80. PMLR, 2018, pp. 1861–1870.

[48] G. Hollinger, S. Singh, J. Djugash, and A. Kehagias, "Efficient multi-robot search for a moving target," *International Journal of Robotics Research (IJRR)*, vol. 28, no. 2, pp. 201–219, 2009.